Inorganica Chimica Acta 377 (2011) 34–41

Contents lists available at SciVerse ScienceDirect

Inorganica Chimica Acta

journal homepage: www.elsevier.com/locate/ica

P-donor ligand containing ruthenium half-sandwich complexes as protein kinase inhibitors

Craig Streu [a], Li Feng [b], Patrick J. Carroll [a], Jasna Maksimoska [a,c], Ronen Marmorstein [a,c], Eric Meggers [a,b,*]

[a] Department of Chemistry, University of Pennsylvania, 231 S., 34th Street, Philadelphia, PA 19104, USA
[b] Fachbereich Chemie, Philipps-Universität Marburg, Hans-Meerwein-Straße, 35043 Marburg, Germany
[c] The Wistar Institute, 3601 Spruce Street, Philadelphia, PA 19104, USA

ARTICLE INFO

Article history:
Received 22 April 2011
Received in revised form 15 July 2011
Accepted 20 July 2011
Available online 30 July 2011

Keywords:
Metal-based drugs
Protein kinases
Inhibitors
Phosphine ligands
Ruthenium

ABSTRACT

Metal complexes have emerged as promising and novel scaffolds for the design of enzyme inhibitors. Reported herein are the design, synthesis, and evaluation of protein kinase inhibition properties of pyridocarbazole half-sandwich complexes containing P-donor ligands. The nature of the monodentate P-donor ligand has a strong effect on protein kinase binding properties, most likely due to a direct interaction with the glycine-rich loop in the ATP-binding site. We furthermore discovered that PMe_3 pyridocarbazole complexes are interesting lead structures for the design of potent inhibitors for the protein kinase TrkA for which we obtained a nanomolar organometallic inhibitor.

1. Introduction

The unique properties of metal complexes such as structural diversity, adjustable ligand exchange kinetics, fine-tuned redox activities, and distinct spectroscopic signatures, render them exciting scaffolds for the design of synthetic compounds with novel biological properties [1]. However, surprisingly, metal-containing compounds play only a minor role in the design of molecular probes for chemical biology or as drug candidates in the pharmaceutical industry [2].

Several years ago we initiated a research program to explore substitutionally inert metal complexes as scaffolds for the design of enzyme inhibitors [3]. Our program is based on the hypothesis that complementing organic elements with typical coordination modes of transition metals such as octahedral or half-sandwich coordination spheres will provide new opportunities for building small molecule structures that might populate unique chemical space which cannot be accessed by purely organic compounds [4]. We primarily focus on metals such as ruthenium, osmium, rhodium, and iridium which are capable of forming kinetically highly stable complexes that are uncompromised in biological environments and should therefore serve as ideal structural metal centers in stable bioactive metal complexes.

For example, we recently reported the promising kinase inhibition and anticancer effects of the metallo-pyridocarbazole complex **DW12** and some of its derivatives (Fig. 1) [5–8]. The ruthenium half-sandwich complex **DW12** is a very selective and potent inhibitor for the protein kinases GSK3 and Pim1 which induces strong biological responses, such as the activation of the Wnt signaling pathway in mammalian cells, strong pharmacological effects during the development of frog embryos, and the efficient induction of apoptosis in some melanoma cell lines. A crystal structure of (*R*)-**DW12** bound to the ATP-binding site of GSK3β provides insight into the important role of the CO ligand for binding affinity of (*R*)-**DW12** to GSK3β [9]: several residues of the glycine-rich-loop – which closes like a lid on top of the inhibitor upon binding – form a small hydrophobic pocket via induced fit that appears perfectly suited for the CO ligand. The unique shape of the organometallic scaffold with the CO ligand oriented perpendicular to the heteroaromatic pyridocarbazole moiety allows the glycine-rich loop to adopt a very close conformation with maximized hydrophobic contacts. This is consistent with our experimental results for this and related organometallic complexes, which demonstrate the importance of the CO group for GSK3 potency and selectivity. Interestingly, published and yet unpublished results accumulated over the last several years suggest that the interaction of different monodentate ligands with the glycine-rich loop can alter protein kinase binding affinity and selectivity significantly [3,10]. This observation is potentially of high relevance since the human genome codes for around 500 protein kinases [11], which all contain

* Corresponding author at: Fachbereich Chemie, Philipps-Universität Marburg, Hans-Meerwein-Straße, 35043 Marburg, Germany.
E-mail address: meggers@chemie.uni-marburg.de (E. Meggers).

0020-1693/$ - see front matter © 2011 Elsevier B.V. All rights reserved.
doi:10.1016/j.ica.2011.07.032

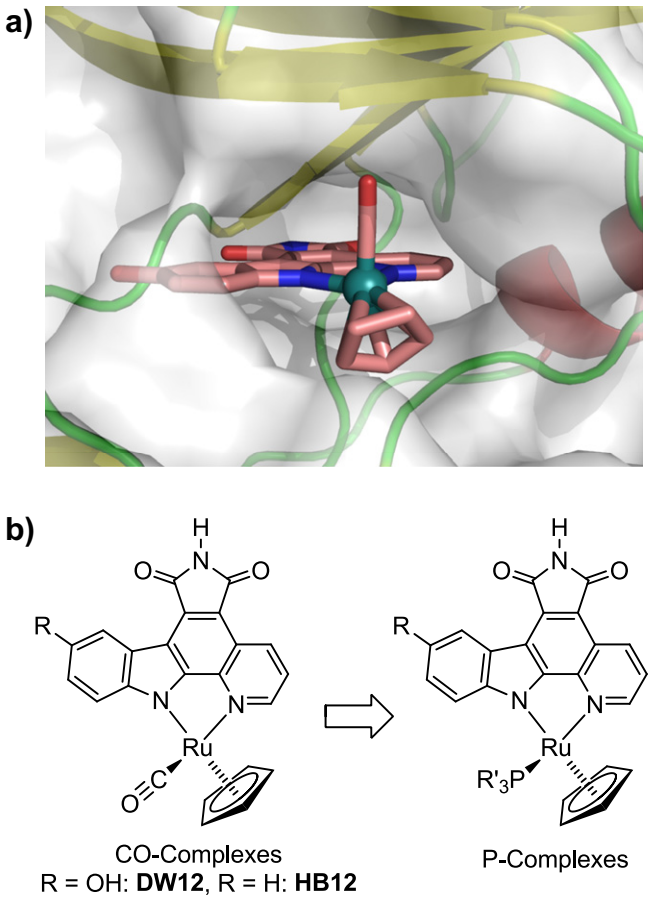

Fig. 1. (a) Binding of the half sandwich complex (*R*)-**DW12** to the ATP-binding site of a protein kinase. (b) Changing the kinase inhibition properties by replacing the CO ligands of **HB12** (R = H) or **DW12** (R = OH) with monodentate P-donor ligands. Only one enantiomer of the CO and PR'_3 complexes are shown.

a highly conserved ATP-binding site, making the design of selective protein kinase inhibitors an extraordinary challenge.

Herein we report the design, synthesis and protein kinase inhibition properties of new organometallic protein kinase inhibitors obtained by replacing the CO ligand of our canonical metallo-pyridocarbazole scaffold by monodentate P-donor ligands.

2. Results and discussion

We started by developing a synthetic route for accessing pyridocarbazole ruthenium half-sandwich complexes bearing monodentate P-donor ligands. The reaction of $[CpRu(CH_3CN)_3]PF_6$ (**1**) [12] with the bidentate pyridocarbazole ligand **2** [13] in the presence of K_2CO_3 in MeCN/MeOH 4:1, followed *in situ* by the addition of PMe_3 afforded the ruthenium half-sandwich complex **3** in this one-pot procedure with a yield of 83% (Scheme 1). Complex **3** is hydrolytically stable. For example, no degradation could be observed by ^1H NMR after three days in DMSO-d_6 and methanol-d_4. The crystal structure of complex **3** is shown in Fig. 2 and confirms the half-sandwich structure of the complex. Crystallographic data are displayed in Table 1. The PMe_3 group is oriented almost perpendicular to the plane of the pyridocarbazole heterocycle as expected for a pseudo-octahedral coordination sphere. However, the phosphine ligand is slightly bent towards the pyridocarbazole heterocycle as can be seen from the bond angles N2–Ru1–P1 = 86.80° and N19–Ru1–P1 = 89.42° (Fig. 2). This might be an important detail since it is most likely this phosphine ligand that

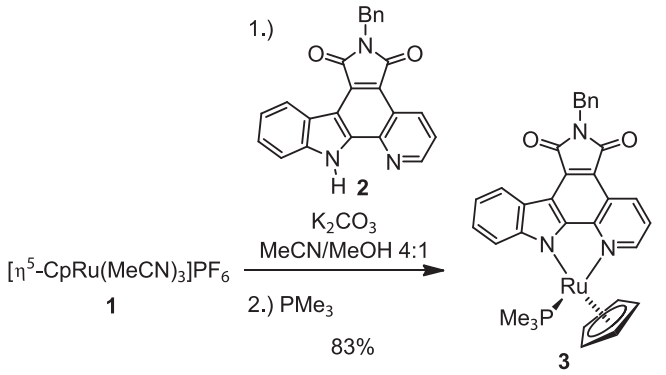

Scheme 1. Single-pot procedure for the synthesis of the racemic phosphine complex **3**.

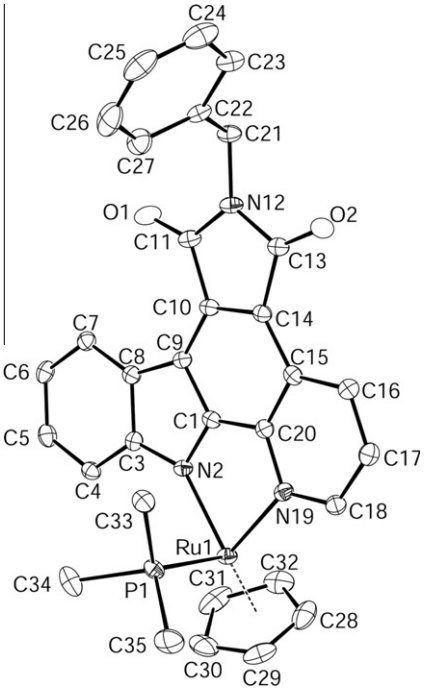

Fig. 2. Crystal structure of PMe_3 complex **3**. ORTEP drawing with 30% probability thermal ellipsoids. Selected bonds distances (Å) and angles (°): Ru1–P1 = 2.2930(9), Ru1–N2 = 2.102(3), Ru1–N19 = 2.140(3), N2–Ru1–N19 = 77.96(10), N2–Ru1–P1 = 86.80(8), and N19–Ru1–P1 = 89.42(8).

interacts with the glycine-rich loop of the ATP-binding site of protein kinases upon binding.

Encouraged by these results, we next synthesized complexes with different P-donor ligands in combination with an unprotected maleimide moiety in order to be able to form important canonical hydrogen bonds to the hinge region of the ATP-binding site. Accordingly, precursor complex **1** was reacted first with *tert*-butyldimethylsilyl (TBS)-protected pyridocarbazole **4** [14] in CH_2Cl_2 at 0 °C in the presence of (−)-sparteine after which the P-ligands PMe_3, PEt_3, $P(CH_2OH)_3$, $P(OMe)_3$, or PF_3 were added to provide complexes **5a**–**e**, followed by removal of the TBS-group with tetrabutylammoniumfluoride (TBAF) to yield complexes **6a** (PMe_3), **6b** (PEt_3), **6c** ($P(CH_2OH)_3$), **6d** ($P(OMe)_3$), and **6e** (PF_3) (Scheme 2). In these reactions, (−)-sparteine gave better results than either K_2CO_3 or Et_3N. All complexes were purified by flash silica gel chromatography. Interestingly, the monodentate ligands have a profound influence on the electronic properties of the ruthenium center as indicated by the different colors of the complexes **6a**,

Table 1
Crystallographic data for complex **3**.

Formula	$C_{32}H_{28}N_3PO_2Ru$
Formula weight	618.61
Crystal class	triclinic
Space group	$P\bar{1}$ (#2)
Z	2
Cell constants	
a (Å)	7.9943(7)
b (Å)	10.5921(9)
c (Å)	16.772(2)
α (°)	105.989(3)
β (°)	91.311(2)°
γ (°)	98.649(2)°
V (Å^3)	1346.7(2)
μ (cm^{-1})	6.77
Crystal size (mm)	0.40 × 0.15 × 0.04
D_{calc} (g cm^3)	1.526
F(0 0 0)	632
Radiation	Mo Kα (λ = 0.71073 Å)
2θ Range (°)	5.06–50.04
hkl Collected	$-9 \leqslant h \leqslant 8$; $-12 \leqslant k \leqslant 12$; $-19 \leqslant l \leqslant 19$
Number of reflections measured	10 950
Number of unique reflections	4716 (R_{int} = 0.0262)
Number of observed reflections	4216 ($F > 4\sigma$)
Number of reflections used in refinement	4716
Number of parameters	356
R indices ($F > 4\sigma$)	R_1 = 0.0408 wR_2 = 0.1039
R indices (all data)	R_1 = 0.0459 wR_2 = 0.1087
Goodness-of-fit (GOF)	1.063
Final difference peaks (e Å^3)	+1.409, −0.787

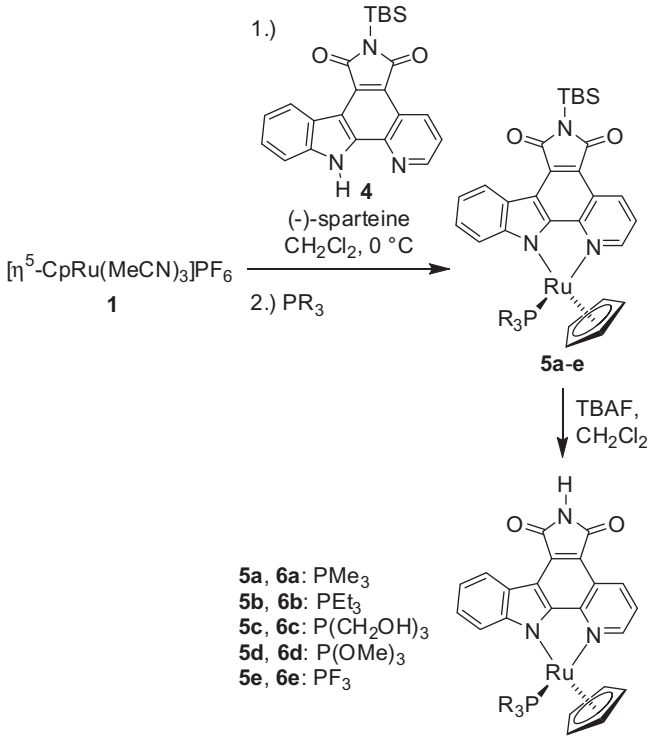

Scheme 2. Synthesis of the racemic P-ligand complexes **6a–e**. See experimental section for individual yields.

6d, and **6e** shown in Fig. 3. As one would expect, complex **6e** bearing a π-acceptor PF_3 ligand comes the closest in color to the solution of **HB12** (Fig. 1) harboring a π-accepting CO ligand.

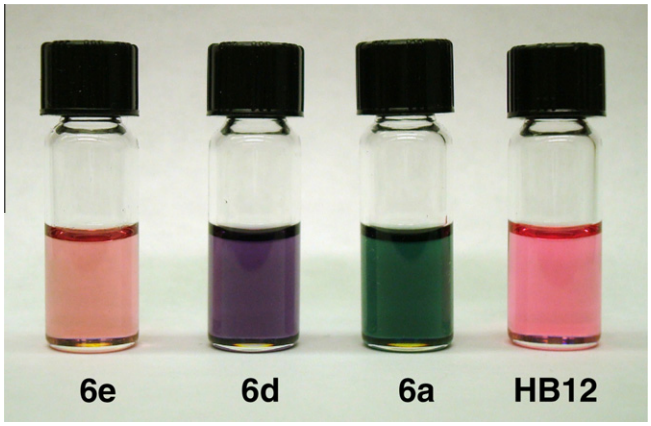

Fig. 3. The different colors of diluted DMSO solutions (100 μM) of the P-ligand complexes **6a** (λ_{max} = 628 nm), **6d** (λ_{max} = 585 nm), and **6e** (λ_{max} = 525 nm) demonstrate the different electronic properties of the P-donor ligands. The color of the CO-containing complex **HB12** (λ_{max} = 535 nm) is shown as a reference. Values for the long-wavelength absorbance maxima are provided in brackets.

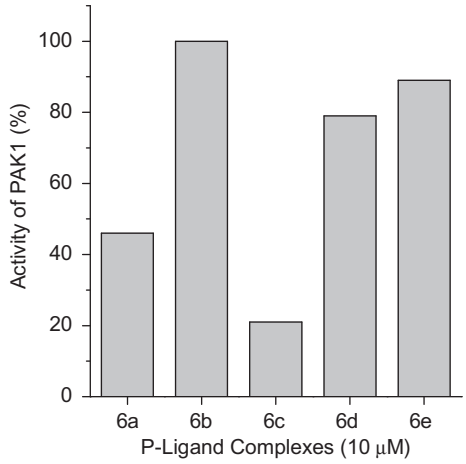

Fig. 4. Inhibition of the protein kinase PAK1 by the P-donor ligand complexes **6a–e** at a concentration of 10 μM and an ATP concentration of 1 μM. The bars represent remaining kinase activities under these conditions.

Since the phosphine ligands are sterically more demanding than the CO ligands of the previous inhibitors **DW12** and **HB12** (Fig. 1), among others, we decided to initially test the complexes **6a–e** as inhibitors for the p21-activated protein kinase 1 (PAK1). PAK1 is distinguished by an especially large ATP binding site which is therefore capable of accommodating more bulky inhibitors [15]. Fig. 4 displays the remaining enzymatic activity of PAK1 in the presence of 10 μM of the individual P-donor ligand complexes **6a–e**. Importantly, the bar diagram demonstrates that the monodentate ligands have a profound effect on the inhibition of PAK1. For example, complex **6b** (100% remaining activity) does not affect the enzymatic activity of PAK1. This is apparently due to the bulkiness of the PEt_3 ligand, which prevents the complex from binding to the ATP-binding site altogether. A related steric effect can explain the weak inhibitory activity of the $P(OMe)_3$ complex **6d** (79% remaining PAK1 activity), whereas the inactivity of the PF_3-complex **6e** (89% remaining PAK1 activity) might be rationalized by an unfavorable interaction of the fluoride ligands with hydrophobic residues of the glycine-rich loop. On the other hand, the small and hydrophobic PMe_3 group of complex **6a** results in a significant inhibition of PAK1 at 10 μM (46% activity). Surprisingly, complex **6c** bearing the $P(CH_2OH)_3$ ligand displays the strongest inhibitory properties (21% remaining PAK1 activity). Apparently

one or more of the OH-groups are involved in additional hydrogen bonds within the ATP binding site of PAK1.

In order to gain additional information about the kinase inhibition properties of this class of P-donor ligand ruthenium half-sandwich complexes, we selected compound **6a** and screened it against a panel of 263 protein kinases. As a result, at a concentration of 1 μM **6a** and 10 μM ATP most protein kinases were not affected by complex **6a**. For example, as shown in the bar diagram of Fig. 5, 103 kinases retained more than 90% of their activities and 197 out of the 263 kinases remained more than 50% active under these conditions. However, the three protein kinases GSK3α, Pim1, and TrkA were almost completely inhibited in the presence of 1 μM of **6a** (<5% activity). Neurotrophic tyrosine kinase receptor type 1 (TrkA), is the high affinity receptor for the nerve growth factor (NGF) [16]. NGF-activated TrkA can promote cell proliferation or differentiation of neurons. Mutations in the gene for TrkA have been associated with several diseases such as mental retardation and cancer. We therefore selected TrkA as a target to design more potent phosphine-based ruthenium inhibitors.

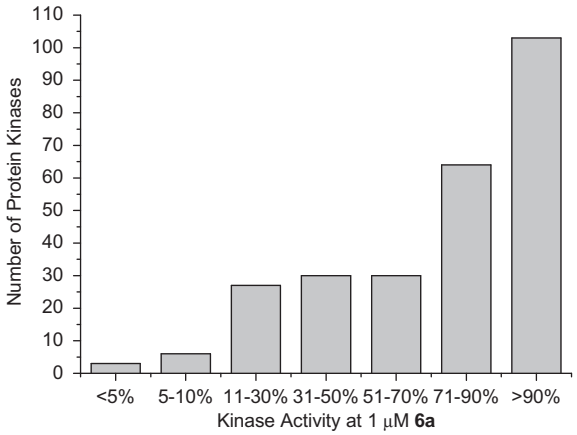

Fig. 5. Selectivity profile of PMe_3 complex **6a** in a panel of 263 protein kinases. Activities were determined by Millipore (KinaseProfiler) at a concentration of 10 μM ATP. Remaining activities are mean values from duplicate measurements. Under these conditions, only three protein kinases show an activity of less than 5% (TrkA, Pim1, GSK3α).

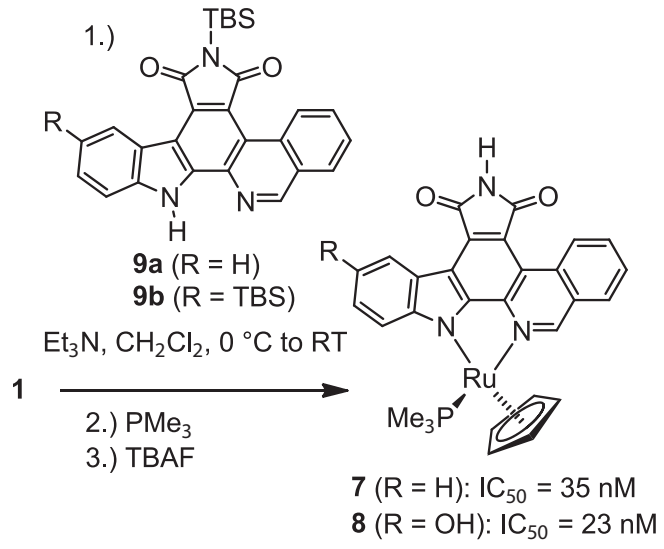

Scheme 3. Synthesis of the racemic TrkA inhibitor **7** and **8**. IC_{50} values against TrkA are shown at 100 μM ATP.

Based on a previous study towards the design of TrkA inhibitors [17], we envisioned that complexes such as **7** and **8**, differing from **6a** by a fused benzene ring at the pyridine moiety and an additional OH-group at the indole 5-position as in **8**, might provide improved TrkA inhibitors (Scheme 3). Complexes **7** and **8** were synthesized in analogy to **6a**–**e** by the reaction of ruthenium precursor complex **1** with TBS-protected pyridocarbazole **9a** [14] or **9b** [17] in the presence of a tertiary amine base, with subsequent addition of PMe_3, followed by a TBS-deprotection with TBAF. As expected, the isoquinoline complex **7** shows an improved IC_{50} value (concentration of inhibitor at which the enzyme activity is reduced to 50%) of 35 nM compared to an IC_{50} of >1 μM for **6a** at the elevated ATP concentration of 100 μM. Additionally, the inclusion of an OH-group at the 5-position of the indole increases the affinity further, rendering complex **8** a highly potent, nanomolar inhibitor for TrkA with an IC_{50} of 23 nM at 100 μM ATP.

3. Conclusions

In conclusion, we have herein reported the design, synthesis and protein kinase inhibition properties of P-donor ligand containing pyridocarbazole half-sandwich complexes. As expected, the nature of the monodentate P-donor ligand has a strong effect on protein kinase binding data, most likely due to a direct interaction with the glycine-rich loop in the ATP-binding site. Finally, we discovered that PMe_3 pyridocarbazole complexes are suitable lead structures for the design of potent TrkA inhibitors and we demonstrated this with the design of a nanomolar inhibitor for TrkA. This work demonstrates that metal complexes are highly suitable structural scaffolds for the design of enzyme inhibitors by using the coordination sphere around the metal center to provide great control over the orientation of ligands within the enzyme active site. Further exploitation of this efficient methodology using novel P-donor ligands may yield potent inhibitors of still new kinases by utilizing otherwise inaccessible regions of chemical space.

4. Experimental

4.1. Materials and methods

Compounds **1** [12], **2** [13], **4** [14], **9a** [14], and **9b** [17] were prepared according to literature procedures. All solvents and reagents were used as supplied from Aldrich, Acros, Strem, and Fisher Scientific. Reactions were performed in oven-dried glassware under an atmosphere of argon unless otherwise noted. Silicycle (250 μm, indicator F254) plates were used for thin layer chromatography and Silia-P Flash silica gel from Silicycle was used for flash chromatography. NMR spectra were recorded on a Bruker AM-500 (500 MHz), DMX-360 (360 MHz), cryo500 (500 MHz), or DMX-300 (300 MHz) spectrometer. NMR standards used are as follows: (^{1}H) $CDCl_3$ = 7.26 ppm, CD_3OD = 3.31 ppm, $(CD_3)_2SO$ = 2.49 ppm, $(CD_3)_2CO$ = 2.05 ppm, CD_3CN = 1.94 ppm. (^{13}C) $CDCl_3$ = 77.23 ppm, $(CD_3)_2SO$ = 39.51 ppm, CD_3CN = 1.32 ppm. High-resolution mass spectra were obtained at the University of Pennsylvania Mass Spectrometry Facility with a Micromass AutoSpec instrument using either chemical or electrospray ionization or with a Waters LCT Premier instrument using electrospray ionization and a TOF analyzer. Infrared spectra were recorded on a Perkin–Elmer 1600 FTIR spectrometer.

4.2. Protein kinase assays

PAK1 was expressed and purified as described elsewhere [15]. TrkA and kinase substrates were purchased from Millipore.

4.2.1. PAK1 assays

Kinase assays were performed using labeled [γ-^{32}P]-ATP and the incorporation of P^{32}-phosphate into the myelin basic protein (MBP) substrate was monitored. Different concentrations of the inhibitors were incubated with 0.2 nM PAK1 kinase in 20 mM MOPS pH 7.0, 30 mM $MgCl_2$, 0.8 μg/μL bovine serum albumin and 5% DMSO (resulting from the inhibitor stock solution) in the presence of 25 μg of MBP substrate for 15 min. Reactions were initiated by adding ATP to a final concentration of 1 μM including 0.2 μCi/μL[γ-^{32}P] ATP in a final volume of 25 μL. The reactions were terminated by spotting 17.5 μL onto circular P81 phosphocellulose paper (diameter 2.1 cm, Whatman), followed by washing three times with 0.75% phosphoric acid and one time with acetone. The dried P81 papers were transferred to scintillation vials and 4 mL of scintillation cocktail was added. The counts per minute (CPM) were measured in a Packard 1500 Tri-Carb Liquid Scintillation Analyzer.

4.2.2. TrkA assays with [γ-^{32}P]ATP

Various concentrations of the measured complexes were incubated at room temperature in 20 mM MOPS, 30 mM $MgCl_2$, 0.8 μg/μL BSA, 5% DMSO (resulting from the inhibitor stock solution), pH 7.0, in the presence of 250 μM Trk peptide KKKSPGEYVNIEFG and 8.0 nM TrkA. After 15 min, the reaction was initiated by adding ATP to a final concentration of 100 μM, including approximately 0.2 μCi/μL [γ-^{32}P]ATP. Reactions were performed in a total volume of 25 μL and incubated at 30 °C. After 45 min, the reaction was terminated by spotting 17.5 μL on a circular P81 phosphocellulose paper (2.1 cm diameter, Whatman), followed by washing four times with 0.75% phosphoric acid and once with acetone. The dried P81 papers were transferred to a scintillation vial, 5 mL of scintillation cocktail was added, and the CPM were determined with a Beckmann 6000 scintillation counter. IC_{50} values were defined to be the concentration of inhibitor at which the CPM was 50% of the control sample, corrected by the background.

4.2.3. TrkA assays with [γ-^{33}P]ATP

Various concentrations of ruthenium complexes were incubated at room temperature in 10 mM MOPS, 10 mM $Mg(OAc)_2$, 0.1 μg/μL BSA, 5% DMSO (resulting from the inhibitor stock solution), pH 7.0, in the presence of 100 μM Trk peptide KKKSPGEYVNIEFG and 10 nM TrkA. After 15 min, the reaction was initiated by adding ATP to a final concentration of 100 μM, including approximately 0.06 μCi/μL [γ-^{33}P]ATP. Reactions were performed in a total volume of 25 μL. After 2 h, the reaction was terminated by spotting 15 μL on a circular P81 phosphocellulose paper (2.1 cm diameter, Whatman), followed by washing three times with 0.75% phosphoric acid and once with acetone. The dried P81 papers were transferred to a scintillation vial, 5 mL of scintillation cocktail was added, and the CPM was determined with a Beckmann 6000 scintillation counter.

4.3. Compound preparation

*4.3.1. Compound **3***

To an argon saturated solution of CH_3CN:MeOH 4:1 (5 mL) at 0 °C, was added benzyl protected pyridocarbazole ligand **2** (43.4 mg, 0.115 mmol) and complex **1** (50.0 mg, 0.115 mmol) to give a dark red solution. After stirring 5 min at 0 °C, K_2CO_3 was added (47.6 mg, 0.345 mmol) causing the reaction to become dark purple. After stirring for 45 min at 0 °C, PMe_3 (35.7 μL, 0.345 mmol) was added and the reaction was allowed to warm slowly to room temperature. After 1 h, the reaction was concentrated and subjected to flash chromatography over silica gel with a 35:1 toluene:acetone mobile phase. The product **3** eluted as a dark green band (59.0 mg, 83%). ^{1}H NMR (500 MHz, $CDCl_3$): δ (ppm) 9.00 (m, 2H, Ar), 8.89 (d, J = 7.9, 1H, Ar), 7.56 (m, 4H, Ar), 7.40–7.32 (m, 4H, Ar), 7.25 (t, J = 7.3, 1H, Ar), 4.96 (s, 2H, NCH_2–C_6H_5), 4.59 (s, 5H, C_5H_5), 0.75 (s, 9H, $P(CH_3)_3$). ^{31}P NMR (122 MHz, $CDCl_3$): δ (ppm) 7.1. IR (film): ν (cm^{-1}) 3054, 2969, 2925, 1744 (C=O), 1691 (C=O), 1579, 1525, 1491, 1415, 1386, 1348, 1262, 1229, 1135, 1100, 1076, 946, 746.

*4.3.2. Compound **5a***

To an argon saturated solution of CH_2Cl_2 (3 mL) at 0 °C, was added ligand **4** (14.3 mg, 0.034 mmol) and precursor complex **1** (15.0 mg, 0.034 mmol) to give a dark solution. After stirring 5 min at 0 °C, (−)-sparteine (10.3 μL, 0.045 mmol) was added causing the reaction to become dark purple. After stirring for 45 min at 0 °C, PMe_3 (31.8 μL, 0.306 mmol) was added and the reaction was allowed to warm slowly to room temperature. After 1 h, the green reaction was concentrated and subjected to flash chromatography over silica gel with a toluene:acetone (50:1) mobile phase. The product **5a** eluted as a dark green band (14.0 mg, 63%). ^{1}H NMR (500 MHz, $CDCl_3$): δ (ppm) 9.06 (d, J = 8.3 Hz, 1H, Ar), 9.02 (d, J = 4.6 Hz, 1H, Ar), 8.89 (d, J = 7.8 Hz, 1H, Ar), 7.54 (m, 2H, Ar), 7.36 (m, 2H, Ar), 4.60 (s, 5H, C_5H_5), 1.07 (s, 9H, $C(CH_3)_3$), 0.77 (br s, 9H, $P(CH_3)_3$), 0.62 (s, 6H, $Si(CH_3)_2$). ^{13}C NMR (125 MHz, $CDCl_3$): δ (ppm) 175.9 (C=O), 175.8 (C=O), 154.7, 153.6, 152.4, 145.2, 132.5, 131.3, 125.6, 125.2, 124.5, 122.1, 121.6, 119.7, 115.9, 115.1, 113.3, 72.6 (C_5H_5), 26.8 ($SiC(CH_3)_3$), 19.4 ($C(CH_3)_3$), 17.9 (d, J_{C-P} = 24 Hz, $P(CH_3)_3$), −3.6 ($Si(CH_3)_2$). ^{31}P NMR (122 MHz, $CDCl_3$): δ (ppm) 7.4. IR (film): ν (cm^{-1}) 2923, 2854, 1676 (C=O), 1587, 1497, 1424, 1399, 1299, 1270, 1219, 1114, 1062, 970, 892, 783, 734. HRMS calcd for $C_{31}H_{37}N_3O_2PRuSi$ $(M+H)^+$ 644.1431, found $(M+H)^+$ 644.1442.

*4.3.3. Compound **6a***

TBS-protected complex **5a** (12 mg, 0.018 mmol) was taken up in dry CH_2Cl_2 (1.5 mL). To this green solution was added a 1.0 M solution of TBAF in THF (27.5 μL, 0.027 mmol) causing the reaction to immediately become purple. After stirring for 40 min, the reaction was quenched by exposing it to acetic acid vapor. The reaction was then concentrated and subjected to flash chromatography over silica gel with a toluene:acetone 25:1 mobile phase. The product **6a** eluted as a dark green band (9.6 mg, 99%). ^{1}H NMR (360 MHz, $CDCl_3$): δ (ppm) 9.03 (m, 2H, Ar), 8.86 (dt, J = 7.9, 1.0 Hz, 1H, Ar), 7.58 (m, 2H, Ar), 7.45 (br s, 1H, NH), 7.43–7.36 (m, 2H, Ar), 4.61 (s, 5H, C_5H_5), 0.77 (d, J_{H-P} = 8.8 Hz, 9H, $P(CH_3)_3$). ^{13}C NMR (90 MHz, $CDCl_3$): δ (ppm) 170.2 (C=O), 170.2 (C=O), 155.0, 153.8, 152.4, 144.9, 130.9, 126.1, 125.1, 124.5, 122.5, 121.9, 121.9, 120.0, 116.0, 115.8, 110.8, 72.7 (C_5H_5), 17.9 (d, J_{C-P} = 26 Hz, $P(CH_3)_3$). IR (film): ν (cm^{-1}) 2963, 2915, 2843, 1743 (C=O), 1695 (C=O), 1575, 1496, 1468, 1416, 1344, 1280, 1260, 1224, 1152, 1097, 1021, 949. HRMS calcd for $C_{25}H_{23}N_3O_2PRu$ $(M+H)^+$ 530.0566, found $(M+H)^+$ 530.0573.

*4.3.4. Compound **5b***

To an argon saturated solution of CH_2Cl_2 (3 mL) at 0 °C, was added ligand **4** (10.0 mg, 0.025 mmol) and precursor complex **1** (11.3 mg, 0.026 mmol) to give a dark solution. After stirring 5 min at 0 °C, (−)-sparteine was added (6.9 μL, 0.030 mmol) causing the reaction to become dark purple. After stirring for 30 min at 0 °C, PEt_3 (11.0 μL, 0.075 mmol) was added and the reaction was allowed to warm slowly to room temperature. After 1 h, the green reaction was concentrated and subjected to flash chromatography over silica gel with a toluene:acetone 50:1 mobile phase. The product **5b** eluted as a dark green band (9.6 mg, 56%). ^{1}H NMR (360 MHz, $CDCl_3$): δ (ppm) 9.06 (d, J = 7.5 Hz, 1H, Ar), 9.05 (d, J = 7.4 Hz, 1H, Ar), 8.90 (ddd, J = 7.9, 1.2, 0.8 Hz, 1H, Ar), 7.62 (d, J = 8.1 Hz, 1H, Ar), 7.54 (m, 1H, Ar), 7.39–7.33 (m, 2H, Ar), 4.58 (s,

5H, C_5H_5), 1.07 (s, 9H, C(CH_3)$_3$), 1.00 (m, 6H, P(CH_2CH_3)$_3$), 0.78 (m, 9H, P(CH_2CH_3)$_3$), 0.62 (s, 3H, SiCH_3), 0.61 (s, 3H, SiCH_3). ^{13}C NMR (90 MHz, $CDCl_3$): δ (ppm) 175.9 (C=O), 175.8 (C=O), 155.0, 153.9, 152.6, 145.5, 132.5, 131.4, 125.5, 125.1, 124.6, 122.0, 121.6, 119.6, 116.0, 115.3, 113.1, 72.4 (C_5H_5), 26.8 (SiC(CH_3)$_3$), 19.4 (SiC(CH_3)$_3$), 17.4 (d, J_{C-P} = 23 Hz, P(CH_2CH_3)$_3$), 7.6 (P(CH_2CH_3)$_3$), −3.6 (Si(CH_3)$_2$). IR (film): ν (cm^{-1}) 2957, 2930, 2852, 1742 (C=O), 1683 (C=O), 1579, 1520, 1495, 1470, 1415, 1338, 1319, 1280, 1259, 1227, 1189, 1174, 1127, 1039, 848, 828, 747, 732. HRMS calcd for $C_{34}H_{42}N_3O_2PRuSi$ (M)$^+$ 685.1827, found (M)$^+$ 685.1805.

4.3.5. Compound **6b**

TBS protected complex **6b** (9.6 mg, 0.014 mmol) was taken up in dry CH_2Cl_2 (1.5 mL). To this was added a 1.0 M solution of TBAF in THF (42 μL, 0.042 mmol) causing the reaction to immediately turn purple. After stirring at room temperature for 5 min, the reaction was quenched by exposing it to acetic acid vapor. The reaction was then concentrated and subjected to flash chromatography over silica gel with toluene:acetone (50:1). The product **6b** eluted as a dark green band (8.0 mg, quant.). ^{1}H NMR (500 MHz, DMSO-d_6): δ (ppm) 10.89 (s, 1H, NH), 9.35 (d, J = 5.2 Hz, 1H, Ar), 8.86 (d, J = 8.3 Hz, 1H, Ar), 8.64 (d, J = 7.9 Hz, 1H, Ar), 7.68 (d, J = 8.2 Hz, 1H, Ar), 7.57 (dd, J = 8.4, 5.1 Hz, 1H, Ar), 7.50 (t, J = 8.1 Hz, 1H, Ar), 7.29 (t, J = 7.8 Hz, 1H, Ar), 4.70 (s, 5H, C_5H_5), 0.94 (m, 6H, P(CH_2CH_3)$_3$), 0.66 (dt, J = 14.6, 7.3 Hz, 9H, P(CH_2CH_3)$_3$). ^{13}C NMR (125 MHz, DMSO-d_6): δ (ppm) 171.0 (C=O), 170.8 (C=O), 154.1, 153.7, 153.2, 144.1, 130.0, 129.5, 125.3, 123.7, 123.4, 122.3, 121.2, 118.9, 116.2, 114.0, 110.7, 72.2 (C_5H_5), 16.6 (d, J_{C-P} = 23 Hz, P(CH_2CH_3)$_3$), 7.2 (P(CH_2CH_3)$_3$). IR (film): ν (cm^{-1}) 3113, 3042, 2966, 2932, 2727, 1742 (C=O), 1700 (C=O), 1579, 1528, 1492, 1418, 1342, 1286, 1260, 1226, 1182, 1126, 1029, 796, 751, 707. HRMS calcd for $C_{28}H_{28}N_3O_2PRu$ (M)$^+$ 571.0963, found (M)$^+$ 571.0969.

4.3.6. Compound **6c**

To an argon saturated solution of CH_2Cl_2 (3 mL) at 0 °C, was added ligand **4** (10.0 mg, 0.025 mmol) and precursor complex **1** (10.8 mg, 0.025 mmol) to give a dark solution. After stirring 5 min at 0 °C, (−)-sparteine was added (6.9 μL, 0.030 mmol) causing the reaction to become dark purple. After stirring for 45 min at 0 °C, P(CH_2OH)$_3$ (9.3 mg, 0.075 mmol) was added and the reaction was allowed to warm slowly to room temperature. After 1 h, the green reaction was concentrated and subjected to flash chromatography over silica gel with a 35:1 CH_2Cl_2:MeOH mobile phase ramped slowly to 15:1 CH_2Cl_2:MeOH. The product **5c** eluted as a blue purple band that also contained sparteine. This residue was taken up in 2 mL of dry CH_2Cl_2. To this solution was added a 1.0 M solution of TBAF in THF (38 μL, 0.038 mmol) causing the reaction color to immediately lighten. After stirring for 5 min at room temperature, the reaction was quenched by exposing it to acetic acid vapor. The reaction was then concentrated and subjected to flash chromatography over silica gel with CH_2Cl_2:MeOH 20:1. The product **6c** eluted as a dark green band that dried to a green solid (3.2 mg, 22% two steps). ^{1}H NMR (500 MHz, $CDCl_3$): δ (ppm) 9.39 (d, J = 5.1 Hz, 1H, Ar), 9.00 (d, J = 8.4 Hz, 1H, Ar), 8.80 (d, J = 7.6 Hz, 1H, Ar), 8.01 (s, 1H, NH), 7.68 (d, J = 8.2 Hz, 1H, Ar), 7.56–7.51 (m, 2H, Ar), 7.34 (t, J = 7.9 Hz, 1H, Ar), 4.81 (s, 5H, C_5H_5), 3.71 (d, J = 13.2 Hz, 3H, P(CH_2OH)$_3$), 3.61 (d, J = 13.2 Hz, 3H, P(CH_2OH)$_3$). IR (film): ν (cm^{-1}) 3410 (br, OH), 3263, 2922, 2852, 1743 (C=O), 1698 (C=O), 1579, 1523, 1493, 1469, 1418, 1343, 1287, 1261, 1227, 1187, 1098, 1076, 1024, 845, 821, 797, 748, 708, 637. HRMS calcd for $C_{26}H_{23}N_3O_5PRu$ (M-CH_3)$^+$ 562.0106, found (M-CH_3)$^+$ 562.0033.

4.3.7. Compound **5d**

To an argon saturated solution of CH_2Cl_2 (3 mL) at 0 °C, was added ligand **4** (17.4 mg, 0.0419 mmol) and precursor complex **1** (20.0 mg, 0.046 mmol) giving a dark solution. After stirring 5 min at 0 °C, (−)-sparteine was added (13.8 μL, 0.060 mmol) causing the reaction to become dark purple. After stirring for 30 min at 0 °C, P(OMe)$_3$ (16.3 μL, 0.138 mmol) was added and the reaction was allowed to warm slowly to room temperature. After 2 h, the reaction was concentrated and subjected to flash chromatography over silica gel with toluene:acetone 50:1. The product **5d** eluted as a dark purple band (10.5 mg). Some TBS-deprotected material **6d** could be eluted as a more polar purple band (1.0 mg) resulting in an overall yield of 43%. ^{1}H NMR (360 MHz, $CDCl_3$): δ (ppm) 9.12 (d, J = 8.1 Hz, 1H, Ar), 9.06 (d, J = 5.2 Hz, 1H, Ar), 8.90 (dt, J = 7.9, 1.1 Hz, 1H, Ar), 7.60 (d, J = 8.2 Hz, 1H, Ar), 7.54 (ddd, J = 8.2, 6.9, 1.3 Hz, 1H, Ar), 7.37 (m, 2H, Ar), 4.81 (s, 5H, C_5H_5), 3.13, (d, J = 11.3 Hz, 9H, P(OCH_3)$_3$), 1.07 (s, 9H, SiC(CH_3)$_3$), 0.62 (s, 6H, Si(CH_3)$_2$). ^{13}C NMR (90 MHz, $CDCl_3$): δ (ppm) 175.9 (C=O), 175.6 (C=O), 155.4, 154.1, 153.8, 145.7, 132.7, 132.4, 125.6, 125.2, 124.5, 121.9, 121.6, 119.6, 115.9, 115.4, 113.5, 75.5 (C_5H_5), 51.2 (OCH_3), 26.8 (SiC(CH_3)$_3$), 19.4 (SiC(CH_3)$_3$), −3.6 (Si(CH_3)$_2$). ^{31}P NMR (122 MHz, $CDCl_3$): δ (ppm) 154.4. IR (film): ν (cm^{-1}) 2947, 2932, 2852, 1742 (C=O), 1685 (C=O), 1581, 1499, 1415, 1338, 1318, 1281, 1228, 1168, 1124, 1021, 828, 747. HRMS calcd for $C_{32}H_{37}N_3O_5PRuSi$ (M+H)$^+$ 692.1278, found (M+H)$^+$ 692.1289.

4.3.8. Compound **6d**

TBS-protected complex **5d** (12.5 mg, 0.018 mmol) was taken up in 2 mL of dry CH_2Cl_2 and cooled to 0 °C. To this was added a 1.0 M solution of TBAF in THF (19.1 μL, 0.019 mmol) causing the reaction to immediately turn red. After stirring for 15 min at 0 °C, the reaction was quenched by exposing it to acetic acid vapor. The reaction was then concentrated and subjected to flash chromatography over silica gel with toluene:acetone 20:1. The product **6d** eluted as a dark purple band that dried to a blue green solid (5.9 mg, 91%) based on recovered starting material. ^{1}H NMR (500 MHz, $CDCl_3$): δ (ppm) 9.07 (m, 2H, Ar), 8.86 (d, J = 7.8 Hz, 1H, Ar), 7.62 (d, J = 8.1 Hz, 1H, Ar), 7.44 (br s, 1H, NH), 7.40 (m, 2H, Ar), 4.83 (s, 5H, C_5H_5), 3.14 (d, J = 11.3 Hz, 9H, P(OCH_3)$_3$). ^{13}C NMR (90 MHz, $CDCl_3$): δ (ppm) 170.2 (C=O), 170.1 (C=O), 155.7, 154.3, 153.8 (d, J_{C-P} = 2.8 Hz), 145.4, 132.1, 131.0, 126.0, 125.2, 124.4, 122.3, 121.8, 119.9, 116.1, 116.0, 111.1, 75.5 (d, J_{C-P} = 3.3 Hz, C_5H_5), 51.3 (d, J_{C-P} = 3.0 Hz, P(OCH_3)$_3$). ^{31}P NMR (122 MHz, $CDCl_3$): δ (ppm) 154.1. IR (film): ν (cm^{-1}) 3207, 3049, 2919, 2854, 1746 (C=O), 1695 (C=O), 1582, 1532, 1491, 1417, 1343, 1287, 1263, 1226, 1152, 1124, 1017, 743. HRMS calcd for $C_{26}H_{23}N_3O_5PRu$ (M+H)$^+$ 578.0413, found (M+H)$^+$ 578.0421.

4.3.9. Compound **5e**

Free ligand **4** (17.4 mg, 0.0419 mmol) and complex **1** (20.0 mg, 0.0461 mmol) were added together to a dry 10 mL two-necked round bottomed flask and placed under argon. The flask was cooled to 0 °C and CH_2Cl_2 (4 mL) was added turning the reaction dark maroon. After stirring 5 min at 0 °C, (−)-sparteine (13.8 μL, 0.060 mmol) was added causing the reaction to become dark purple. After stirring for 45 min at 0 °C, the reaction was purged with freshly generated PF_3 gas using argon as a carrier gas, while slowly warming to room temperature. During this time, the reaction became deep red. After 2 h, the reaction was concentrated and subjected to silica gel chromatography with toluene:acetone 50:1. The product **5e** eluted as a bright red band (10.5 mg). Some TBS-deprotected material (**6e**) could be eluted as a more polar purple band (1.0 mg) resulting in an overall yield of 43%. ^{1}H NMR (360 MHz, $CDCl_3$): δ (ppm) 9.26 (dt, J = 8.3, 1.1 Hz, 1H, Ar), 8.88 (m, 2H, Ar), 7.57 (ddd, J = 8.4, 7.0, 1.3 Hz, 1H, Ar), 7.47 (dd, J = 8.3, 5.1 Hz, 1H, Ar), 7.41 (m, 2H, Ar), 5.14 (d, J = 1.3 Hz, 5H, C_5H_5),

1.06 (s, 9H, SiC(CH_3)$_3$), 0.62 (s, 6H, Si(CH_3)$_2$). ^{13}C NMR (90 MHz, $CDCl_3$): δ (ppm) 175.7 (C=O), 175.1 (C=O), 155.1, 154.4 (d, J_{C-P} = 3.4 Hz), 153.4, 145.2, 134.5, 133.2, 126.3, 125.5, 124.5, 122.1, 122.1, 120.1, 115.9, 115.2, 114.5, 79.0 (d, J_{C-P} = 4.3 Hz, C_5H_5), 26.7 (SiC(CH_3)$_3$), 19.4 (SiC(CH_3)$_3$), -3.7 (Si(CH_3)$_2$). ^{31}P NMR (122 MHz, $CDCl_3$): δ (ppm) 134 (q, J_{P-F} = 1341 Hz). IR (film): ν (cm^{-1}) 2926, 2854, 1740 (C=O), 1688 (C=O), 1586, 1504, 1416, 1337, 1262, 1229, 1180, 1127, 1046, 849 (P–F), 747, 663, 576. HRMS calcd for $C_{28}H_{28}F_3N_3O_2PRuSi$ (M+H)$^+$ 656.0679, found (M+H)$^+$ 656.0687.

4.3.10. Compound **6e**

TBS-protected complex **5e** (10.5 mg, 0.016 mmol) was taken up in dry CH_2Cl_2 (2 mL) and cooled to 0 °C. To this was added tetrabutylammonium fluoride (1.0 M solution in THF) (17.6 μL, 0.018 mmol) causing the reaction to immediately turn purple. After stirring for 3 min at 0 °C, the reaction was quenched by exposing it to acetic acid vapor. The reaction was then concentrated and subjected to silica gel chromatography with toluene:acetone 10:1. The product **6e** eluted as a light purple band (4.0 mg, 46%). ^{1}H NMR (500 MHz, DMSO-d_6): δ (ppm) 11.07 (s, 1H, NH), 9.28 (d, J = 5.0 Hz, 1H, Ar), 9.09 (d, J = 8.2 Hz, 1H, Ar), 8.66 (d, J = 7.9 Hz, 1H, Ar), 7.75 (dd, J = 8.4, 5.1 Hz, 1H, Ar), 7.55 (m, 2H, Ar), 7.35 (ddd, J = 8.0, 5.5, 2.5 Hz, 1H, Ar), 5.44 (s, 5H, C_5H_5). ^{13}C NMR (125 MHz, $CDCl_3$): δ (ppm) 169.9 (C=O), 169.6 (C=O), 155.3, 154.6 (d, J_{C-P} = 2.6 Hz), 153.5, 144.8, 134.2, 131.5, 126.7, 125.4, 124.3, 122.4, 122.3, 120.5, 116.5, 115.3, 112.2, 79.0 (d, J_{C-P} = 3.8 Hz, C_5H_5). ^{31}P NMR (122 MHz, $CDCl_3$): δ (ppm) 134 (q, J_{P-F} = 1341 Hz). IR (film): ν (cm^{-1}) 3192, 2920 , 2854 , 1746 (C=O), 1700 (C=O), 1581, 1538, 1519, 1494, 1460, 1417, 1343, 1291, 1262, 1229, 1151, 1011, 854 (P–F), 741. HRMS calcd for $C_{22}H_{14}F_3N_3O_2PRu$ (M+H)$^+$ 541.9814, found (M+H)$^+$ 541.9816.

4.3.11. Compound **7**

To an argon saturated solution of CH_2Cl_2 (2 mL) was added ligand **9a** (10.0 mg, 0.022 mmol) and ruthenium precursor **1** (10.0 mg, 0.023 mmol) as solids to give a dark solution. After stirring for 5 min at 0 °C, (−)-sparteine was added (6.6 μL, 0.029 mmol) causing the reaction to turn dark purple. After stirring for 45 min at 0 °C, a 1.0 M solution of PMe_3 in THF (66 μL, 0.066 mmol) was added and the reaction was allowed to warm slowly to room temperature. After 1 h, the green reaction was concentrated and subjected to flash chromatography over silica gel with a hexanes:EtOAc 10:1. The TBS protected product of this reaction was concentrated to a green solid (4.9 mg) that was carried forward without characterization. To a solution of the TBS protected complex (4.9 mg, 0.007 mmol) in CH_2Cl_2 (2 mL) at 0 °C was added a 1.0 M solution of TBAF in THF (19.0 μL, 0.019 mmol) causing the reaction to immediately become red colored. After stirring for 15 min at 0 °C, the reaction was quenched with 1 drop of HOAc. The reaction was then concentrated and subjected to flash chromatography over silica gel with toluene:acetone 10:1. The product **7** concentrated to a green solid (2.4 mg, 59%). ^{1}H NMR (500 MHz, $CDCl_3$): δ (ppm) 10.55 (d, J = 9.0 Hz, 1H, Ar), 9.63 (s, 1H, Ar), 9.03 (d, J = 7.8 Hz, 1H, Ar), 7.96 (t, J = 7.5 Hz, 1H, Ar), 7.79 (t, J = 5.8 Hz, 1H, Ar), 7.61 (t, J = 7.6 Hz, 1H, Ar), 7.53 (m, 2H, Ar), 7.39 (m, 2H, Ar and NH), 4.65 (s, 5H, C_5H_5), 0.83 (d, J = 8.5 Hz, 9H, P(CH_3)$_3$). ^{13}C NMR (125 MHz, DMSO-d_6): δ (ppm) 171.1 (C=O), 170.5 (C=O), 157.2, 154.6, 153.8, 139.7, 130.8, 130.7, 130.1, 128.8, 128.1, 127.7, 126.4, 125.3, 124.6, 123.1, 119.9, 118.5, 115.9, 115.7, 112.5, 72.8 (d, J_{C-P} = 2.4 Hz, C_5H_5), 16.7 (d, J_{C-P} = 25.8 Hz, P(CH_3)$_3$). IR (film): ν (cm^{-1}) 3121, 3056, 2961, 2921, 2850, 2741, 1743 (C=O), 1696 (C=O), 1618, 1579, 1533, 1462, 1423, 1380, 1328, 1293, 1227, 1123, 1022, 814, 758. HRMS calcd for $C_{29}H_{24}N_3O_2PRu$ (M)$^+$ 579.0650, found (M)$^+$ 579.0861.

4.3.12. Compound **8**

To a N_2-saturated solution of CH_2Cl_2/MeCN (2 mL/0.4 mL) were added ligand **9b** (30 mg, 0.048 mmol) and ruthenium complex **1** (25.1 mg, 0.058 mmol) as solids. After stirring for 5 min at 0 °C, N,N-diisopropylethylamine (10 μL, 0.058 mmol) was added. The mixture was allowed to warm to room temperature and stirred overnight. A 1 M solution of PMe_3 in THF (144 μL, 0.144 mmol) was added to the purple solution. After 1 h, the green solution was concentrated and subjected to flash chromatography over silica gel with hexanes:EtOAc (first 10:1, then 8:1). The product was concentrated to a green solid (18.5 mg) that was carried forward without characterization. To a solution (5.2 mg) in CH_2Cl_2 (2 mL) at 0 °C was added a 1 M solution of TBAF in hexane (18 μL, 0.018 mmol). After stirring for 5 min at 0 °C, the reaction was quenched with one drop of glacial acetic acid. The solution was then concentrated and subjected to flash chromatography over silica gel with CH_2Cl_2:MeOH (first 100:1, then 50:1). The complex **8** was concentrated to a green solid (2.9 mg, 36% over both steps). ^{1}H NMR (400 MHz, DMSO-d_6): δ (ppm) 11.04 (s, 1H, NH), 10.47 (d, J = 8.6 Hz, 1H, Ar), 9.96 (d, J = 2.1 Hz, 1H, Ar), 9.05 (s, 1H, OH), 8.28 (d, J = 2.4 Hz, 1H, Ar), 8.23 (d, J = 7.8 Hz, 1H, Ar), 7.95 (t, J = 8.2 Hz, 1H, Ar), 7.84 (t, J = 7.7 Hz, 1H, Ar), 7.42 (d, J = 8.6 Hz, 1H, Ar), 7.09 (dd, J = 8.6, 2.5 Hz, 1H, Ar), 4.74 (s, 5H, C_5H_5), 0.74 (d, J_{H-P} = 9.1 Hz, 6H, P(CH_3)$_3$). ^{13}C NMR (100.6 MHz, DMSO-d_6): δ (ppm) 171.0 (C=O), 170.5 (C=O), 156.6 (d, J_{C-P} = 4.1 Hz), 154.3, 150.8, 147.9, 139.9, 131.1, 130.4, 130.1 (d, J_{C-P} = 0.9 Hz), 128.7, 127.9, 127.7, 127.6 (d, J_{C-P} = 2.1 Hz), 123.5, 119.7, 116.4, 115.9, 115.8, 110.9, 109.3, 72.7 (d, J_{C-P} = 2.3 Hz, C_5H_5), 16.7 (d, J_{C-P} = 25.7 Hz, P(CH_3)$_3$). IR (film): ν (cm^{-1}) 3419 (br, OH), 3127, 2925, 2853, 1741 (C=O), 1694 (C=O), 1678, 1581, 1492, 1464, 1335, 947, 756. HRMS calcd for $C_{29}H_{25}N_3O_3PRu$ (M+H)$^+$ 596.0679, found (M+H)$^+$ 596.0666.

4.4. X-ray crystallography

Single crystals suitable for X-ray diffraction studies were grown by slow diffusion of pentane into a solution of **3** in chloroform. This complex, $C_{32}H_{28}N_3PO_2Ru$, crystallized in the triclinic space group $P\bar{1}$ with a = 7.9943(7) Å, b = 10.5921(9) Å, c = 16.772(2) Å, α = 105.989(3)°, β = 91.311(2)°, γ = 98.649(2)°, V = 1346.7(2) Å^3, Z = 2 and d_{calc} = 1.526 g/cm^3. X-ray intensity data were collected on a Rigaku Mercury CCD area detector employing graphite-monochromated Mo Kα radiation (λ = 0.71073 Å) at a temperature of 143 K. Preliminary indexing was performed from a series of twelve 0.5° rotation images with exposures of 60 s. A total of 830 rotation images were collected with a crystal to detector distance of 35 mm, a 2θ swing angle of −10°, rotation widths of 0.5° and exposures of 30 s: scan no. 1 was a ϕ-scan from 52.5° to 262.5° at ω = 10° and ω = 20°; scan no. 2 was an ω-scan from −20° to 20° at χ = −90° and ϕ = 135°; scan no. 3 was an ω-scan from −20° to 4° at χ = −90° and ϕ = 315°; scan no. 4 was an ω-scan from −20° to 8° at χ = −90° and ϕ = 225°. Rotation images were processed using CrystalClear, producing a listing of unaveraged F^2 and $\sigma(F^2)$ values which were then passed to the CrystalStructure program package for further processing and structure solution on a Dell Pentium III computer. A total of 10950 reflections were measured over the ranges $5.06 \leqslant 2\theta \leqslant 50.04°$, $-9 \leqslant h \leqslant 8$, $-12 \leqslant k \leqslant 12$, $-19 \leqslant l \leqslant 19$ yielding 4716 unique reflections (R_{int} = 0.0262). The intensity data were corrected for Lorentz and polarization effects and for absorption using REQAB (minimum and maximum transmission 0.824, 1.000). The structure was solved by direct methods (SIR97). Refinement was by full-matrix least squares based on F^2 using SHELXL-97. All reflections were used during refinement (F^2's that were experimentally negative were replaced by F^2 = 0). The weighting scheme used was $w = 1/[\sigma^2(F_o^2) + 0.0595P^2 + 1.5778P]$ where $P = (F_o^2 + 2F_c^2)/3$. Non-hydrogen atoms were refined anisotropically and hydrogen

atoms were refined using a "riding" model. Refinement converged to $R_1 = 0.0408$ and $wR_2 = 0.1039$ for 4216 reflections for which $F > 4\sigma(F)$ and $R_1 = 0.0459$, $wR_2 = 0.1087$ and GOF = 1.063 for all 4716 unique, non-zero reflections and 356 variables. The maximum Δ/σ in the final cycle of least squares was 0.001 and the two most prominent peaks in the final difference Fourier were +1.409 and −0.787 e Å^3. Table 1 lists cell information, data collection parameters, and refinement data.

Acknowledgements

We would like to thank Prof. Jeffrey D. Winkler (Department of Chemistry, University of Pennsylvania) for generously providing equipment and facilities as well as his helpful discussions on the topic. We would also like to thank Dr. Nicholas Pagano for assistance with the TrkA assay.

Appendix A. Supplementary material

Supplementary data associated with this article can be found, in the online version, at doi:10.1016/j.ica.2011.07.032.

References

[1] (a)For metal complexes with bioactivities, see for example: C. Orvig, M.J. Abrams (Eds.)Chem. Rev. 99 (1999) 2201;
(b) Z. Guo, P.J. Sadler, Angew. Chem., Int. Ed. 38 (1999) 1512;
(c) W.H. Ang, P.J. Dyson, Eur. J. Inorg. Chem. (2006) 4003;
(d) T.W. Hambley, Science 318 (2007) 1392;
(e) R. Alberto, J. Organomet. Chem. 692 (2007) 1179;
(f) T.W. Hambley, Dalton Trans. (2007) 4929;
(g) E. Meggers, Chem. Commun. (2009) 1001;
(h) C.L. Davies, E.L. Dux, A.-K. Duhme-Klair, Dalton Trans. (2009) 10141;
(i) C.G. Hartinger, P.J. Dyson, Chem. Soc. Rev. (2009) 38, 391;
(j) R.H. Fish, Aust. J. Chem. 63 (2010) 1505;
(k) E.A. Hillard, G. Jaouen, Organometallics 30 (2011) 20;
(l) G. Gasser, I. Ott, N. Metzler-Nolte, J. Med. Chem. 54 (2011) 3.
[2] This is for example illustrated by a review of drugs approved by the US Food and Drug Administration during 2007 in which not a single compound contains a metal atom. See: B. Hughes, Nat. Rev. Drug Discov. 7 (2008) 107.
[3] For a very recent example, see: L. Feng, Y. Geisselbrecht, S. Blanck, A. Wilbuer, G.E. Atilla-Gokcumen, P. Filippakopoulos, K. Kräling, M.A. Celik, K. Harms, J. Maksimoska, R. Marmorstein, G. Frenking, S. Knapp, L.-O. Essen, E. Meggers, J. Am. Chem. Soc. 133 (2011) 5976.
[4] E. Meggers, Curr. Opin. Chem. Biol. 11 (2007) 287.
[5] D.S. Williams, G.E. Atilla, H. Bregman, A. Arzoumanian, P.S. Klein, E. Meggers, Angew. Chem., Int. Ed. 44 (2005) 1984.
[6] G.E. Atilla-Gokcumen, D.S. Williams, H. Bregman, N. Pagano, E. Meggers, ChemBioChem 7 (2006) 1443.
[7] J.É. Debreczeni, A.N. Bullock, G.E. Atilla, D.S. Williams, H. Bregman, S. Knapp, E. Meggers, Angew. Chem., Int. Ed. 45 (2006) 1580.
[8] K.S.M. Smalley, R. Contractor, N.K. Haass, A.N. Kulp, G.E. Atilla-Gokcumen, D.S. Williams, H. Bregman, K.T. Flaherty, M.S. Soengas, E. Meggers, M. Herlyn, Cancer Res. 67 (2007) 209.
[9] G.E. Atilla-Gokcumen, L. Di Costanzo, E. Meggers, Biol. Inorg. Chem. 6 (2011) 45.
[10] H. Bregman, P.J. Carroll, E. Meggers, J. Am. Chem. Soc. 128 (2006) 877.
[11] G. Manning, D.B. Whyte, R. Martinez, T. Hunter, S. Sudarsanam, Science 298 (2002) 1912.
[12] T.P. Gill, K.R. Mann, Organometallics 1 (1982) 485.
[13] H. Bregman, D.S. Williams, G.E. Atilla, P.J. Carroll, E. Meggers, J. Am. Chem. Soc. 126 (2004) 13594.
[14] (a) (a) H. Bregman, D.S. Williams, E. Meggers, Synthesis (2005) 1521.;
(b) N. Pagano, J. Maksimoska, H. Bregman, D.S. Williams, R.D. Webster, F. Xue, E. Meggers, Org. Biomol. Chem. 5 (2007) 1218.
[15] J. Maksimoska, L. Feng, K. Harms, C. Yi, J. Kissil, R. Marmorstein, E. Meggers, J. Am. Chem. Soc. 130 (2008) 15764.
[16] S.O. Meakin, E.M. Shooter, Trends Neurosci. 15 (1992) 323.
[17] N. Pagano, E.Y. Wong, T. Breiding, H. Liu, A. Wilbuer, H. Bregman, Q. Shen, S.L. Diamond, E. Meggers, J. Org. Chem. 74 (2009) 8997.